LUMPED PARAMETER APPROACH APPLIED TO SURFACE FIRE SPREAD MODELING

Rodolfo Maduro Almeida, rodolfo@lac.inpe.br
Graduate Program in Applied Computing, National Institute for Space Research, Sao Jose dos Campos – SP – Brazil

Elbert Einstein Nehrer Macau, elbert@lac.inpe.br
Fernando Manuel Ramos, fernando@lac.inpe.br
Computing and Applied Mathematics Laboratory, National Institute for Space Research, Sao Jose dos Campos – SP – Brazil

Issamu Muraoka, issamu@dem.inpe.br
Space Mechanics and Control Division, National Institute for Space Research, Sao Jose dos Campos – SP – Brazil

Abstract. *This work presents a new approach for surface wildland fire spread behavior modeling based on lumped parameter approach. The fuel bed is decomposed into a finite number of regions called nodes. Each node has a specific temperature, thermal capacitance and an internal heat generation mechanism. Each node exchanges heat with its neighbors through conductive conductances and with the flames and ambient through radiative conductances. When the node reaches the ignition temperature an internal heat generation mechanism, that represents the heat produced during the combustion, remains whereas the fuel into the node is consumed. The flame over each burning node is represented by a parallelepiped whose surfaces emits thermal radiation to the surrounding nodes. Each flame has a temperature-time profile model, length, tilt angle and a residence time over the node. A differential equation system represent the net heat balance of the nodes. The system is numerically solved, yielding, among other results, the temporal evolution of the fire front propagation over the fuel bed. Simulations are carried out for evaluate the model.*

Keywords*: lumped parameter approach, surface fire spread model, forest fire*

1. INTRODUCTION

A wildland fire is an uncontrolled fire that consumes a forest. The knowledge of wildland fire behavior is an important ingredient in fire management decision-making such as prescribed fire planning and fire suppression strategies (Pyne et al., 1996). Fire spread models are mathematical models that integrate information about the main set of environmental factors directly related with fire behavior such as vegetation, topography and weather, and are used for predict the advance of the fire front over the surface with a certain level of confidence (Pastor et al., 2003). The computer implementation of these models and the integration with geographical information systems have made a qualitative leap forward in the development of powerful computational tools for decision-making support in fire management, such as the BEHAVE (Andrews et al., 2003) and the FARSITE (Finney, 2004) systems.

According to the nature of equations, the fire spread models are classified as (Pastor et al., 2003): (i) theoretical models (Morvan and Dupuy, 2001), generated from the laws that govern fluid mechanics, combustion and heat transfer; (ii) empirical models (Hargrove et al., 2000), composed of statistical correlations extracted from experiments or historical wildland fire studies; (iii) semi-empirical models (Rothermel, 1972), proposed from simple, general and theoretical expressions, and completed through experimentation. Although the theoretical approach tries to model the fire spread with a physical-chemical rigor, nevertheless they were not free from empirical components which were indispensables to complete these models. Recently, there is a tendency for use of the theoretical simplified models (Morandini et al., 2005), whose equations represent the main heat transfer mechanisms and they use some empirical correlations that simplify a lot of chemical and thermodynamic questions related to fire behavior.

In this work we purpose a theoretical simplified model. The mathematical formulation is based on lumped parameter approach. According with this approach, the thermal domain of the problem is decomposed into a finite number of lumps called nodes. This discretization process ignores the spatial variation of the dependent variable and the system is described by a set of first order differential equations which model the net flow heat of the nodes. The thermal-electrical analogy assumes that the heat flux between the nodes is like an electric current with an associated resistance (or conductance) where the temperature is the driving factor. Thus, the Ohm's law can be applied to model heat flux and conductances describe the heat transfer mechanisms. The main advantages of the lumped parameter approach are the simplicity in the model formulation, relative precision and efficiency in the processing time (Gilmore and Collins, 1994).

This work is divided in four parts. In the first part, we discussed about the surface fire spread in wildland fires. In the second part the details of the approach is discussed. In the penultimate part a set of results of simulations experiments are presented. In the last part we discussed the conclusions and future works.

2. THE DYNAMICS OF SURFACE FIRE SPREAD IN WILDLAND FIRES

We can identify three main regimes of fire propagation in forest fires, according to the main fuel layers that are involved in the combustion process: (i) ground fire, (ii) surface fire, and (iii) crown fire (Pyne et al., 1996). We are interested in the surface fire spread regime. During a surface fire spread, a wide of class of vegetation litter, dead and live fine fuels at or near the soil surface, is consumed in a flaming combustion. This complex of wildland fuels consumed by fire is here called fuel bed. The region of fuel bed which there are intense flames and a large quantity of heat is released constitutes the called fire front.

The surface fire spread modeling cannot be considered as definitively resolved with conclusive solutions, but it is one of the fields which have provided the most basic notions of wildland fire dynamics (Pastor et al., 2003). A portion of the heat released in the fire front is transmitted to fuel bed situated ahead the fire front heating it, generating a process of pyrolysis (visible charring) followed of flaming combustion. The pyrolysis occurs when the fuel bed particles, which are composed predominantly of cellulose, are heated and they expel its moisture content (water vapor), CO_2, CO and others subproducts (Ward, 2001). One of the main subproducts is the levoglucosan, a volatile that supports the flaming combustion. To interact with oxygen in the air, the levoglucosan composes a flammable gaseous mixture that to the reach a temperature greater than or equal about 600 K, ignites and burns in flaming combustion. In this moment appear the flame, and a large quantity of heat is released, inducing the particles inside the flaming combustion zone to a self-sustained pyrolysis followed of flame combustion that remains as the fuel is consumed.

The dynamics of the surface fire spread is governed by three main heat transfer mechanisms which are: convection and radiation (Pyne et al., 1996). The convection occurs when the hot gases from the fire front flow into the fuel bed and interact with the surface of leaves, branches, shrubs, grass, etc. The geometric properties of these fuel bed components (size and shape) have a fundamental importance in the heat transfer by convection in wildland fires (Morvan and Dupuy, 2001). The radiation is very important heat transfer mechanism in forest fire, given the high temperatures that are reached in the reaction zones of the fire. The thermal radiation occurs when a radiant heat flux is emitted from the fire front to this surrounding. According (Viegas, 1998), there are two combustion zones in the fire front: one inside the solid porous fuel bed and other in the gaseous phase, in the flame above the fuel bed. Whereas the radiation emitted from the solid phase has a short range limited to the internal part of fuel bed nearest the fire front, the radiation emitted from the flames above the fuel bed has a long range and is of paramount importance for surface fire spread. The radiant heat flux from the flame impinges the fuel bed components situated ahead the fire front heating it. The radiation from the flame depends greatly on the geometric properties of the flame such as length and inclination angle in relation to fuel bed surface (Viegas, 1998).

The physical factors that have significant influence on the development of a forest fire are usually grouped in three main categories that are: topography, vegetation and weather (Pyne et al., 1996). Among the various physical factors, the effects of the wind and slope are the most important for changes in the heat transfer mechanisms related to fire spread (Rothermel, 1972). In general, the wind aided and/or upslope fire spread show highest rates of spread when compared with no-wind and no-slope conditions. This increase in the rate of spread is caused by the intensification of the heat transfer mechanisms by radiation and convection because the reduction of the distance between the flames and the surface of fuel bed (Pyne et al., 1996). Therefore, the fire spread most quickly in the upslope and wind directions (Pyne et al., 1996; Viegas, 1998).

3. LUMPED PARAMETER APPROACH MODELING APPLIED TO SURFACE FIRE SPREAD

In this section we attempt to present the main details of the surface fire spread modeling approach. We assume that radiation emitted from the flames are the main heat transfer mechanism to fire spread and which a heat diffusion mechanism represent the radiation and convection heat transfer mechanism that occurs inside the fuel bed. The fuel bed constitutes by a set of identical, cylindrical and thermally thin particles randomly distributed over the surface. The particles have the same surface area to volume ratio σ_p(m^2/m^3), density ρ_p (kg/m^3), specific heat c_p (J/kg/K) and moisture content M_p(-). The fuel bed has a depth δ (m), a fuel load w_0 (kg/m^2), a density $\rho_b = w_0/\sigma$ (kg/m^3) and packing ratio $\beta = \rho_b/\rho_p$ (-).

Based on assumptions, in principle, we idealize the fire front spreading across a fuel bed of depth δ e can represent the fuel bed thermal behavior by the following conservation energy equation:

$$\rho_p c_p \frac{\partial T}{\partial t} = \kappa \nabla^2 T + \dot{q} \tag{1}$$

where the κ (W/m/K) is the fuel bed effective thermal conductivity and $\dot{q}$ (W/m^3) is internal heat production which represent the energy production during the combustion.

The Equation 1 is submitted to following boundary conditions:

$$\begin{cases} z = 0 \Rightarrow -\kappa\, \partial T/\partial t = 0, \\ z = \delta \Rightarrow -\kappa\, \partial T/\partial t = q''_{rad-a} + q''_{rad-f}. \end{cases} \tag{2}$$

which means to say that for $z = \delta$, the fuel bed upper surface, occurs heat exchanges by radiation with the immediately above gases, denoted by q''_{rad-a}, and with the flames, denoted by q''_{rad-f}.

The basis of the lumped parameter approach is the discretization to thermal domain into a finite number of lumps called nodes. Here, we consider two kinds of nodes: the *fuel bed nodes*, which are obtained by the fuel bed discretization, and the *flame nodes*, which represent the flame situated above a burning fuel bed. Each fuel bed node has the dimensions Δx, Δy e $\Delta z = \delta$. If the fuel bed node belongs to fire front, a parallelepiped whose surfaces emit thermal radiation represents the flame node above it. The Figure 1 illustrates the thermal domain discretization and thermal conductances for a node positioned ahead the fire front. The fuel bed is decomposed into 36 nodes (6×6) and three nodes composes the fire fronts. The pathways depict the thermal conductances of node i, and the illustration exhibits four diffusive conductances and four radiative conductances (three between the node and the flames and one between the node and the immediately above gases).

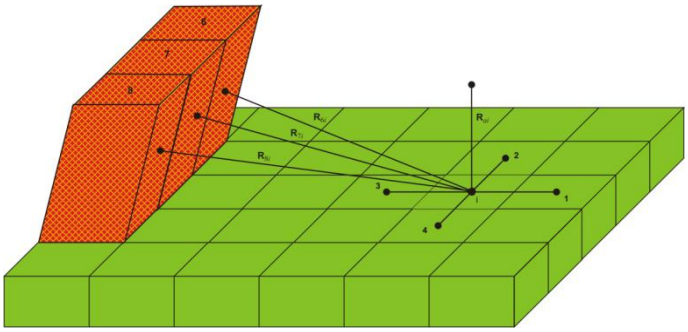

Figure 1: Illustration of the thermal domain decomposition and representation of fire front.

The finite difference method provides the basis for converting a distributed parameter model (Equation 1) into a lumped parameter model. The finite difference approximations for the partial derivatives and after the integral over the volume $V = \Delta x \cdot \Delta y \cdot \Delta z$ are applied in the Equation 1. We assume that there are not internal gradients of temperature inside the nodes. The originated equation expresses the thermal balance of a node i.

The first term of the equation assumes the form:

$$\int_V \rho_p c_p \frac{\partial T}{\partial t} dV \approx \rho_p c_p \frac{\partial T_i}{\partial t} \Delta x \Delta y \Delta y = m_i c_p \frac{dT_i}{dt}, \tag{3}$$

where m_i and T_i are, respectively the fuel mass and temperature of flame node i.

Using centered finite differences approximations the diffusion term of Equation 1 assumes the form:

$$\int_V \kappa \nabla^2 T dV \approx \kappa \frac{T_{x-\Delta x} - T_x}{\Delta x} \Delta y \Delta z + \kappa \frac{T_{x+\Delta x} - T_x}{\Delta x} \Delta y \Delta z + \\ + \kappa \frac{T_{y-\Delta y} - T_y}{\Delta y} \Delta x \Delta z + \kappa \frac{T_{y+\Delta y} - T_y}{\Delta y} \Delta x \Delta z + \int_x \int_y \int_{z=0}^{\delta} \frac{\partial}{\partial z} \left(\frac{\partial T}{\partial z} \right) dx dy dz. \tag{4}$$

Using the index j for represent the nearest neighbors nodes of the node i, and denoting $A_{j,i}$ and $L_{j,i}$ as, respectively, the cross-sectional area between and the distance the centers of the nodes j and i, we obtain the following expression:

$$\int_V \kappa \nabla^2 T dV \approx \sum_{j=1}^{N} \kappa A_{j,i} \frac{T_j - T_i}{\mathrm{L_{j,i}}} + \int_x \int_y \int_{z=0}^{\delta} \frac{\partial}{\partial z} \left(\frac{\partial T}{\partial z} \right) dx dy dz. \tag{5}$$

Substituting the boundary conditions for $z = 0$ and $z = \delta$ in the Equation 5, and considering that the radiant heat exchanges occur between surfaces we obtain the following expressions:

$$\int_V \kappa \nabla^2 T dV \approx \sum_{j=1}^{N} \kappa A_{j,i} \frac{T_j - T_i}{\mathrm{L_{j,i}}} + \left(k \frac{\partial T}{\partial z}\bigg|_{z=\tau} - k \frac{\partial T}{\partial z}\bigg|_{z=0} \right) \Delta x \Delta y \tag{6}$$

$$\int_V \kappa \nabla^2 T dV \approx \sum_{j=1}^{N} \kappa A_{j,i} \frac{T_j - T_i}{\mathrm{L_{j,i}}} = \Delta y \Delta z + \sum_{k=1}^{N} \sigma_{SB} A_i F_{k+N,i} (T_{k+N}^4 - T_i^4), \tag{7}$$

where the index k denotes the burning nodes, N the number of fuel bed nodes, $k + N$ is the flame node above the burning node k, A_i the upper surface area of the node i, and $F_{k+N,i}$ the view factor between the surface of flame node above $k + N$ and the upper surface area of the node i. The integral of the term $\dot{q}$ from Equation 1 over the volume $V = \Delta x \cdot \Delta y \cdot \Delta z$ is represented by Q_i and represents the internal heat generation of heat of the node i.

Substituting into the Equation 1 the expressions obtained previously, we obtain the following set of first order differential equations that represent the net heat transfer rate of the nodes:

$$C_i \frac{dT_i}{dt} = \sum_{j=1}^{N} B_{j,i} \frac{T_j - T_i}{\mathrm{L_{j,i}}} + \sum_{k=1}^{N} R_{j,i} (T_{k+N}^4 - T_i^4) + Q_i \qquad (i = 1,2, \dots, N), \tag{8}$$

where, for a given fuel bed node i, $C_i = m_i c_p$ is its thermal capacitance; T_i is its temperature; B_{ji} the diffusive conductances between the node and its nearest neighbor fuel bed nodes represented by the index j; $R_{k+N,i}$ the radiative conductances between its upper surface area and the surface area of flame above the burning node k, which is represented by the index $k + N$, and between its surface area and immediately above gases; and Q_i its internal heat generation term. The Equation (1) stipule that the rate of variation of internal energy of the node i (first term), is equals to the heat exchanged to nearest neighbors through diffusive conductances (second term), plus the energy rate exchanged by radiation through radiative conductances (third term), plus the internal heat generation term (fourth term).

The diffusive conductance is given by the expression:

$$B_{ji} = \begin{cases} 0, & \text{if } j \text{ is not adjacent to } i \\ \dfrac{k_b A_{ji}}{L_{ji}}, & \text{if } j \text{ is adjacent to } i \end{cases} \tag{9}$$

where k_b (W/m/k) is the effective thermal conductivity of the fuel bed; A_{ji} is the cross sectional area ($A_{ji} = \delta \cdot \Delta x$ or $A_{ji} = \delta \cdot \Delta y$) and L_{ji} the distance between the center of nodes j and i. We suppose that the heat diffusion inside the fuel bed is the aggregate effect of a parallel arrangement of heat diffusion in the solid phase (fuel bed particles) and gaseous phase (air between the fuel bed particles), and the effective thermal conductivity is given by $k_b = (1 - \beta) k_{ar} + \beta k_p$, where k_{ar} and k_p are, respectively, the air thermal conductivity and the fuel bed particles thermal conductivity.

The radiative conductance between the flame node $k + N$ and the fuel bed node i is given by the expression:

$$R_{k+N,i} = \begin{cases} 0, & \text{if } k \text{ is not burning} \\ \sigma_{SB} A_i F_{i,k+N}, & \text{if } k \text{ is burning} \\ \sigma_{SB} A_i, & \text{if } k = i \text{ (radiate exchanges with immediately above surrounding gases)} \end{cases} \tag{10}$$

where $\sigma_{SB} = 5.67 \times 10^{-8}$ $\mathrm{Wm^{-2}K^{-4}}$ is the Stefan-Boltzmann constant, $A_i = \Delta x \cdot \Delta y$ is the upper surface area of the fuel bed node, and $F_{i,k+N}$ is the view factor[1] between the upper surface area A_i and the node flame surface area.

Fire behavior models provides the estimation of the parameters which describes the flame node behavior, such as: the geometric properties length L (m) and inclination angle in relation to vertical θ (°) (Andrews et al., 2003); residence time above the fuel bed node which burns, the same as the fuel bed node combustion time, τ_r (s) (NelsonJr, 2003); and a temperature-time profile (maximum flame temperature T_{Fmax} (K) and curves for temperature raise and fall) which represent the flame node temperature during the combustion (Cruz, 2004). After past the fuel bed node combustion time, the flame node and the heat generation term disappear.

The internal heat generation rate is given by the expression:

$$Q_i = \begin{cases} 0, & \text{if } i \text{ is not burning} \\ -H \dfrac{dm_i(t)}{dt}, & \text{if } i \text{ is burning} \end{cases} \tag{11}$$

where H (J/kg) is the fuel heat of combustion and corresponds to a quantity of energy released resulting from complete combustion of one quantity of fuel mass, the fuel loss rate during the combustion is approximated by the asymptotic

[1] The view factor F_{ij} indicates the proportion of all radiation which leaves surface i and impinges the surface j. See (Incropera and Dewitt, 2003) for more information.

decreasing curve $m_i(t) = m_i(0) \cdot \exp((t - t_{ig})/W)$ which varies in function of the time since the ignition instant time t_{ig} (s) and the constant W define the fuel loss rate intensity. To obtain the value of W we assume that for $t^* - t_{ig} = \tau_r$, the fuel bed node remaining mass is only residual solid carbon (char). The char fraction γ_c (-) determines this remaining proportion (Nelson, 2003).

4. SIMULATIONS AND RESULTS

The computational model is based on library PCTER (Bastos, 1990). The PCTER is library of subroutines written in FORTRAN language developed by the National Institute for Space Research (Brazil) for satellite thermal design. This design is based on lumped parameter approach, wherein PCTER library includes subroutines for calculate the thermal conductances and solve the set of first order differential equation of system thermal behavior.

4.1 Experimental data and node flame behavior

For the simulations, we use experimental data extracted from fire spread experiments using wood excelsior2. These data and the thermal, physical and chemical properties of this fuel can be obtained in the references (Catchpole et al., 1998; Nelson, 2003; Forest Products Laboratory, 1999). The fuel bed surface is supposed horizontal and flat with dimensions width = 20.2 meters, length = 20.2 meters and depth $\delta = 0.10$ meters. The fuel bed is decomposed into a set of 101 × 101 fuel bed nodes where $\Delta x = \Delta y = 0.20$ meters and $\Delta z = \delta$. We use the line ignition initial conduction, where in $t = 0$ s, the fuel bed nodes situated in one fuel bed border are ignited. The solution of Equation 1 gives the fuel bed node temperature in each time instant t. The Table 1 summarizes the model input variables utilized in the simulations. In the simulations we desire analyze the influence of variation in wind speed U (m/s) on fire behavior quantify by the model. We use two different values of wind speed: $U = 0.5$ m/s and $U = 1.0$ m/s. The estimated flame node behavior parameters for these two scenarios are show in the Table 2.

Table 1. Model input parameters.

Fuel bed particles properties	
Specific heat	$c_p = 1400$ J/Kg/K
Density	$\rho_p = 398$ kg/m^3
Surface are to volume ratio	$\sigma_p = 3092$ m^2/m^3
Heat content	$H = 19600$ kJ/kg
Moisture content	$M_p = 0.05$
Char fraction	$\gamma_c = 0.15$
Thermal conductivity	$k_p = 0.11$ W/m/k
Ignition temperature	$T_{ig} = 600$ K
Fuel bed properties	
Fuel load	w_0 =0.5 and 1.0 kg/m^2
Depth	$\delta = 0.1$ m
Fuel bed discretization	$\Delta x = \Delta y = 0.20$ cm and $\Delta z = \delta$
Weather	
Atmosphere temperature	$T_{amb} = 300$ K
Wind speed	$U = 0.5$, 1.0 and 1.5 m/s
Wind direction	

Table 2. Estimated flame node behavior for the two simulated spread scenarios.

Scenario	w_0 (kg/m^2)	U (m/s)	L (m)	θ (°)	τ_r (s)	T_{Fmax} (K)
1	0.5	0.5	0.99	11.95	26.43	1016.90
2	0.5	1.0	1.27	19.40	26.12	1057.36

Comparing the results of scenarios 1 and 2 from Table 2, we can observe that when the wind speed increases, the flame tilt angle and length increases, the residence time decreases and the maximum flame temperature increases. When higher is the wind speed, most higher is the combustion efficiency, due to the fact that more oxygen impinges the burning zone and thus, most heat is released during the burning. These aspects can be observed with the increase of maximum flame temperature and decrease of residence time. The flame geometry is the resultant of two induced flows that exists inside the flame: a buoyancy induced flow due the low density combustion products released in the reaction

zone and wind-induced flow (Viegas, 1998). Thus, when higher is the wind speed, higher will be wind-induced flux and consequently the flame tilt angle in relation to vertical increases. When the quantity of heat released increases, the buoyancy induced flow increases, and consequently the flame length so increases.

4.2 Model convergence and performance analysis

According to (Gilmore and Collins, 1994), the use of lumped parameter approach requires approximations (thermal domain discretization) that results in errors. These errors can be reduced with a fine discretization, but it generates a large number of fuel bed nodes which increases the model computational performance, once the dimension of the first order differential equation system (Eq. 1) increase. Thus, the ideal solution for the problem is the equilibrium between convergence and performance. In this section we analyze the influence of the discretization on the model behavior and the computational performance.

The fire rate of spread is a physical variable which depends of the combined effect of a set of factors that includes vegetation, weather and topography. Thus, the model can calculated this value independently of the thermal domain discretization. In the model, the rate of spread is computed by the fire front advance over the fuel bed in function of the time. We compute the rate of spread for the simulation of the fire spread for scenario 2 using different levels of discretization for a mesh of equally spaced fuel bed nodes with dimensions $\Delta x = \Delta y = \Delta s$. The results are showed in the Table 3.

Table 3. Model convergence analysis results.

Discretization level	Fire rate of spread
$\Delta s = 1.50$ m	$R = 0.1575$ m/s
$\Delta s = 1.00$ m	$R = 0.1731$ m/s
$\Delta s = 0.75$ m	$R = 0.1875$ m/s
$\Delta s = 0.60$ m	$R = 0.2041$ m/s
$\Delta s = 0.50$ m	$R = 0.2212$ m/s
$\Delta s = 0.40$ m	$R = 0.2308$ m/s
$\Delta s = 0.30$ m	$R = 0.2356$ m/s
$\Delta s = 0.20$ m	$R = 0.2416$ m/s
$\Delta s = 0.15$ m	$R = 0.2394$ m/s
$\Delta s = 0.10$ m	$R = 0.2424$ m/s

We observe in the results from Table 3 that as the discretization is refined, the fire rate of spread converges to a value around $R = 0.24$ m/s. Thus, we can verify the method convergence. The flame nodes geometric properties (which depends of the discretization level) has fundamental importance in this convergence process because the radiation from the flames above the burning fuel bed nodes is the main heat transfer mechanism. In the Figure 2 we plot the fire rate of spread in function of the relative height - discretization level ratio ($L \cdot cos\ \theta / \Delta s$).

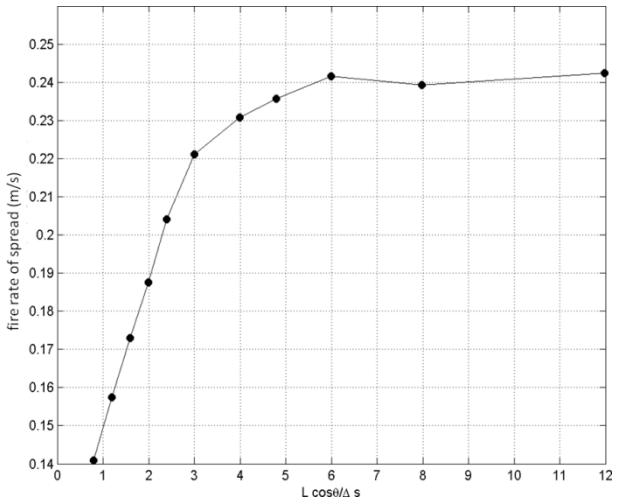

Figure 2: Fire rate of spread convergence.

A better discretization level do not imply in a good computer performance. A fine mesh generates a model with a high number of nodes and conductances (system size), that require an elevated computer performance for solve the first order differential equation system (Eq. 1). In the performance analysis, we carry out simulations for the scenario 2 with line ignition and using a fuel bed of dimensions 10 meters × 10 meters with different refined meshes. For each discretization level we compute the time necessary for the fire front travel the entire fuel bed. These simulations are carried out in a PC Computer with processor AMD Athlon XP 2300+ 1.8 GHz processor and with 1 GB of RAM memory. The Table 4 shows the results.

Table 4. Computational model performance analysis results.

Mesh dimensions (system size)	Δs	Processing time
10×10 (100 fuel bed nodes)	$\Delta s = 1.00$ m	2.15 sec
20×20 (400 fuel bed nodes)	$\Delta s = 0.50$ m	20.01 sec
40×40 (1600 fuel bed nodes)	$\Delta s = 0.25$ m	2 min 51 sec
50×50 (250 fuel bed nodes)	$\Delta s = 0.20$ m	5 min 44 sec
100×100 (10,000 fuel bed nodes)	$\Delta s = 0.10$ m	51 min 25 sec
125×125 (15,625 fuel bed nodes)	$\Delta s = 0.08$ m	1h 41 min 15 sec

We can observe in the Table 3 that the computer performance decreases as the system size increases. The Figure 3 shows, in logarithmic scale, the processing time in function of the system size. The line fitted to performance data has angular coefficient of 1.5717. The following power-law expresses this relation between the processing time t_{proc} (s) and the system size N (number of nodes): $t_{proc} \propto N^{1.5717}$.

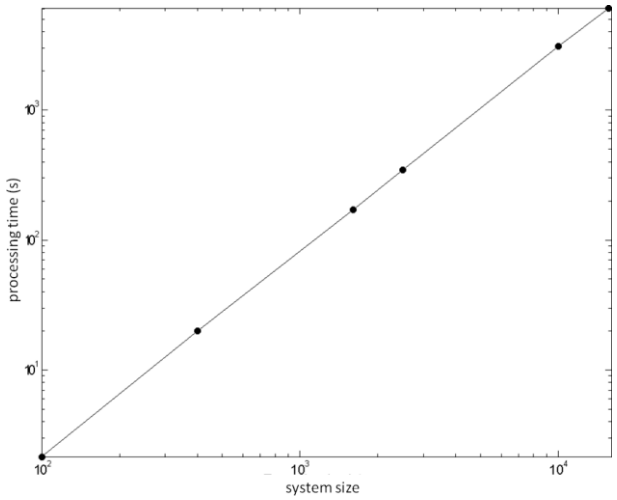

Figure 3: Logarithmic scale plot for time processing in function of the system size.

4.2 Model convergence and performance analysis

The Figure 4 shows the temperature distribution for t = 10 s and t = 80 using input parameters specified in the Table 1 to the scenario 2. The white lines are the isotherm for $T_i = T_{ig}$ and represent the fire front boundaries. Starting for a line ignition in the left fuel bed border for $t = 0$ s, the fire spreads and for $t = 80$ s the fire front is near to the right fuel bed border. From the time instant in which the fuel bed node temperature reaches the ignition temperature it begins to burn. An internal heat generation mechanism occurs for represent the heat produced during the combustion. The term Q_i in the Equation 1 represent this mechanism and the heat produced is directly proportional to fuel loss rate and keeps as the fuel is consumed. The Figure 5 (a) shows the remaining fuel mass of a fuel bed node during the fire spread. Before the ignition, the fuel mass is constant. During the combustion the remaining fuel mass decreases exponentially during the time interval determined by τ_r. After the combustion, the remaining fuel mass is only the char fraction of the initial fuel mass. The fire front gradient temperature observed in the Figure 4 can be most detailed in the Figure 5 (b) which shows the temperatures of the fuel bed node and of the flame node above it, after, during and before the combustion. The Figure 5 (b) shows the model capability is characterize the phases of combustion: preheating, ignition, combustion and extinction (Pyne et al., 1996). As the fire front is nearing the node temperature rises. In this stage, the surrounding

air temperature is equal the atmosphere temperature. When reaches the ignition temperature, the thermal behavior of the surrounding air is calculated by the flame temperature-time profile model. After the combustion, the surrounding air temperature can be the atmosphere temperature and the node temperature decreases until reach the atmosphere temperature. The surrounding air temperature during the combustion is modeled by the temperature-time profile model. The flame node temperature starts from T_{ig} and increases until reaches T_{Fmax} and after decreases until T_{ig}. The shapes of the temperature rising and fall curves are conform proposed in (Cruz, 2004).

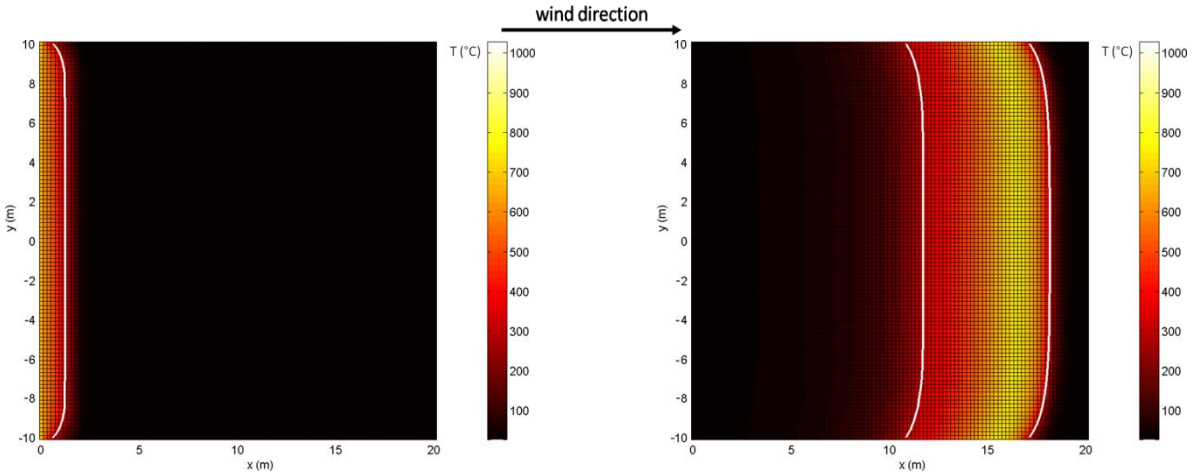

(a) scenario 1, $t = 10$ s (b) scenario 1, $t = 80$ s

Figure 4: Fuel bed temperature distribution for scenario 1 during the fire spread for $t = 0$ s and $t = 60$ s.

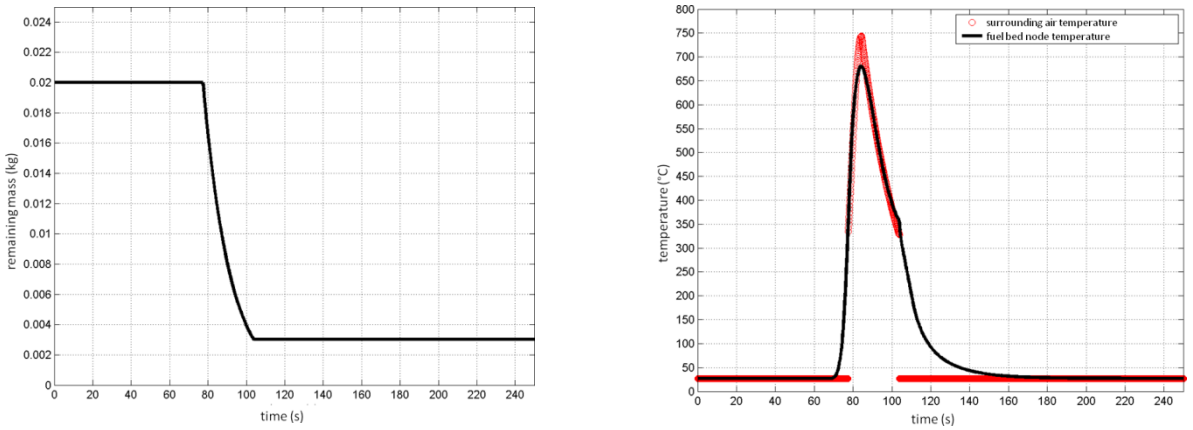

(a) remaining fuel mass (b) fuel bed node and surrounding air temperatures

Figure 5: (a) Remaining fuel mass and (b) fuel bed node and surrounding air temperatures during the fire spread for scenario 1.

The Figure 6 compares the temperature distribution in a same time for the scenarios 1 and 2. For a same time t = 60 seconds, we observe the different fire front positions for the two simulated scenarios. For the scenario 2, increase in the wind speed imply in an increase in the fire rate of spread. It occurs because the increase in the radiant heat flux due the shortening of the distance between the flames and the nodes situated ahead the fire front. This effect is observed in the Figure 7, which shows the view factor contour lines for one flame node positioned in $x = 0$ and $y = 0$. We can observe that the view factor contour lines for both scenarios are most intensified in the wind direction. For the scenario 2, where the wind speed is greater than scenario 1, this intensification is higher. These deformations of contour lines increases in the wind direction as the wind speed increases. Consequently, the radiant heat flux emitted from the flame node to the fuel bed nodes in this region is most intense and thus, the fire spreads most quickly in this direction. It is the effect of wind speed represented in the proposed model and we can verify that the flame node geometric properties are directly related to fire behavior.

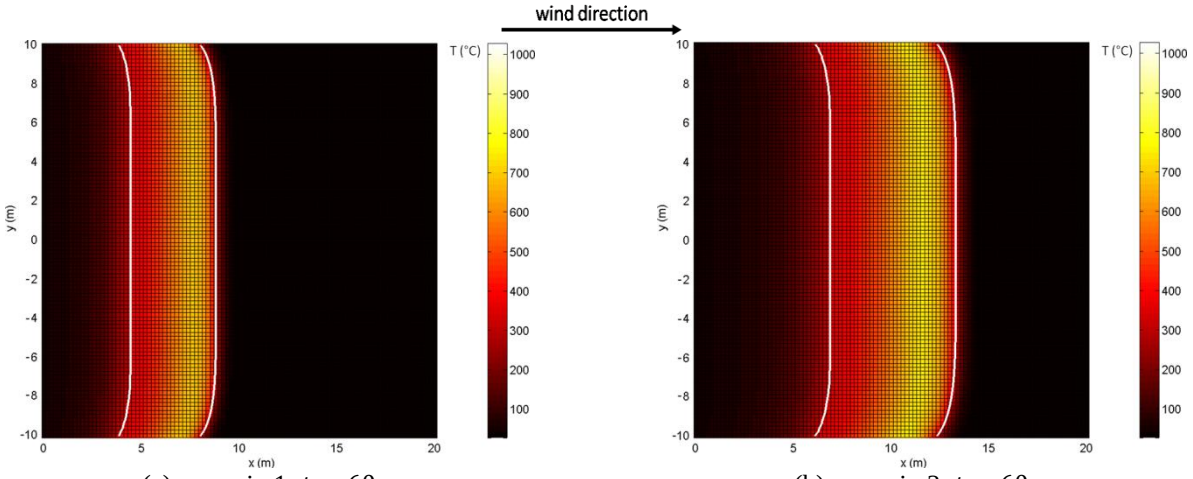

(a) scenario 1, $t = 60$ s (b) scenario 2, $t = 60$ s

Figure 6: Comparison of the fuel bed temperature distribution for scenarios 1 and 2 during the fire spread for $t = 60$ s.

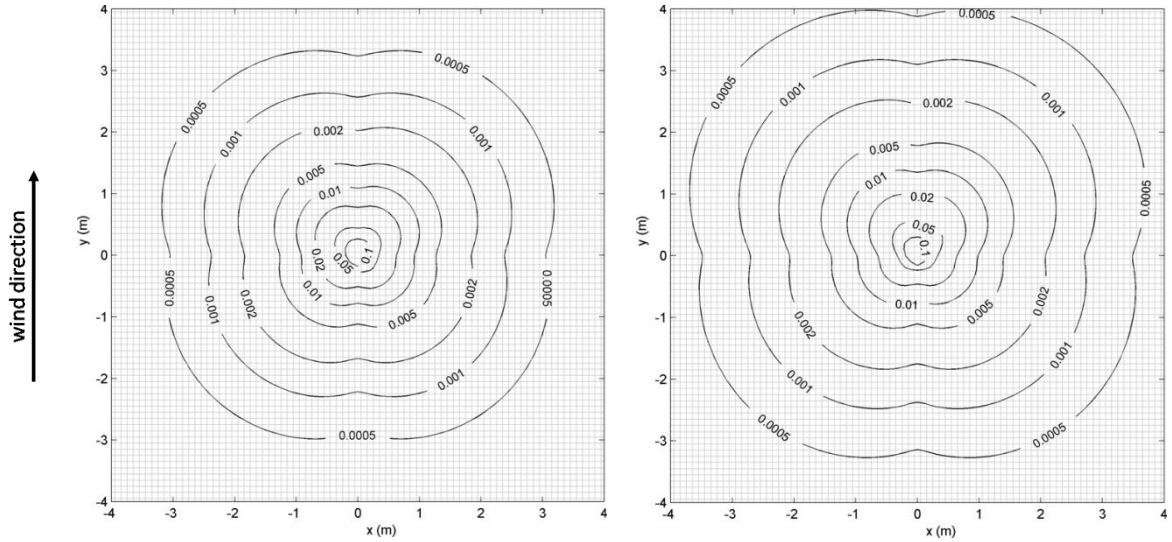

(a) scenario 1 (b) scenario 2

Figure 7: View factor contour lines for the view factor calculated between a flame node positioned in $x = 0$ and $y = 0$ and the neighbors fuel bed nodes for the scenarios 1 and 2. White squares represent the fuel bed node upper surface. In the figure the wind blows from bottom to up.

5. CONCLUSIONS

In this paper, a lumped parameter model for surface fire spread simulated and evaluated. We verify that the numerical method converges for a problem solution and we analyze the processing time in relation to system size. The proposed model can describe the phases of combustion namely preheating, ignition, combustion and extinction. The scenarios simulations for different wind speed values reveal the model capability in include the wind effects on fire propagation. We verify that flame geometric properties have fundamental importance in the fire behavior once we assume which the fire spread is primarily governed by the radiation emitted from the fire front. This model is in development phase, and the first results encourage the use of the lumped parameter approach in fire spread modeling.

6. ACKNOWLEDGEMENTS

This work is sponsored by *Coordenação de Aperfeiçoamento de Pessoal de Nível Superior* (CAPES), *Conselho Nacional de Desenvolvimento Científico e Tecnológico* (CNPq) and *Fundação de Amparo à Pesquisa do Estado de São Paulo* (FAPESP).

7. REFERENCES

Andrews, P. L., Bevins, C. D., Seli, R. C., 2003, "BehavePlus fire modeling system, version 2.0 – User's Guide", Gen. Tech. Rep. RMRS-GTR-106WWW, Ogden, UT: USDA Forest Service, Intermountain Forest and Range Experiment Station.

Bastos, J. L. F., Muraoka, I., Cardoso, H., 1990, "Pacote de análise térmica PCTER". In: Anais do I Simpósio Brasileiro de tecnologia aeroespacial, São José dos Campos, SP: Instituto Nacional de Pesquisas Espaciais (INPE), pp. 256 – 257.

Catchpole, W.R., Catchpole, E.A., Rothermel, R.C., Morris, G.A., Butler, B.W., Latham, D.J., 1998. "Rate of spread of free-burning fires in woody fuels in a wind tunnel", Combust. Sci.Technol 131, 1-37.

Cruz M. G, 2004, "Ignition of crown fuels above a spreading surface fire", PhD Thesis, University of Montana, Missoula, MT, USA.

Finney M. A., 2004, "FARSITE (Fire Area Simulator): model development and evaluation". Research Paper RMRS-RP-4, Missoula, MT: USDA Forest Service, Rocky Mountain Research Station.

Forest Products Laboratory, 1999, "Wood Handbook: wood as an engineering material", Gen. Tech. Rep. FPL-GTR-113, Madison , WI: U.S. Department of Agriculture, Forest Service, Forest Products Laboratory.

Gilmore D. G., Collins R. L., "Thermal design analysis", In: Gilmore D. G. (Ed.), "Satellite thermal control handbook", El Segundo, CA: The Aerospace Corporation Press.

Hargrove W. W., Gardner R. H., Turner M. G., Romme W. H., Despain D. G., 2000, "Simulating fire patterns in heterogeneous landscapes", Ecological Modeling, v. 135, n. 2/3, pp. 243–263.

Incropera F. P., Dewitt D. P., 2002, "Fundamentals of heat and mass transfer", John Wiley & Sons.

Morandini F., Simeoni A., Santoni P. A., Balbi, J. H., 2005, "A model for the spread of fire across a fuel bed incorporating the effects of wind and slope", Combustion Science and Technology, v. 177, n. 7, p. 1381–1418.

Morvan D., Dupuy J. L., 2001, "Modeling of fire spread through a forest fuel bed using a multiphase formulation", Combustion and flame, v. 127, n.1-2, pp. 1981-1994.

Pastor E., Zárate L., Arnaldos J., 2003, "Mathematical models and calculation systems for the study of wildland fire Behavior". Progress in Energy and Combustion Science, v. 29, n. 2, pp. 139-153.

Pyne J. S., Andrews P. L., Laven R. D., 1996, "Introduction to wildland fire", 2. ed., New York, NY: John Wiley & Sons.

NelsonJr R. M., 2003, "Reaction times and burning rates for wind tunnel headfires", International Journal of Wildland Fire, v. 12, n. 2, pp. 195–211.

Rothermel R. C., 1972, "A mathematical model for predicting fire spread in wildland fuels", Research Paper INT-115, Ogden, UT: US Department of Agriculture, Forest Service, Intermountain Forest and Range Experiment Station.

Vidyasagar M., Anderson B. D. O., 1989, "Approximation and stabilization of distributed systems by lumped systems", Systems & Control Letters, v 12, n. 2, pp. 95-101.

Viegas D. X, 1998, "Forest fire propagation". Phil. Trans. R. Soc. Lond. A, v. 356, n. 1748, pp. 2907–2928.

Ward, D., 2001, "Combustion chemistry and smoke", In: Johnson, E. A.; Miyanishi, K. (Ed.), Forest fires: behaviour and ecological effects, San Diego, CA: Academic Press, p. 55–77.

5. RESPONSIBILITY NOTICE

The authors are the only responsible for the printed material included in this paper.